Evaluation of white matter microstructure in patients with Parkinson's disease using microscopic fractional anisotropy

メタデータ	言語: English 出版者: 公開日: 2020-03-20 キーワード (Ja): キーワード (En): 作成者: 池之内, 穣 メールアドレス: 所属:
URL	https://jair.repo.nii.ac.jp/records/2002485

Evaluation of white matter microstructure in patients with Parkinson's disease using microscopic fractional anisotropy

Yutaka Ikenouchi 1, Koji Kamagata 2, Christina Andica 1, Taku Hatano 3, Takashi Ogawa 3, Haruka Takeshige-Amano 3, Kouhei Kamiya 4, Akihiko Wada 1, Michimasa Suzuki 1, Shohei Fujita 1, Akifumi Hagiwara 1, Ryusuke Irie 4, Masaaki Hori 1, Genko Oyama 3, Yashushi Shimo 5, Atsushi Umemura 6, Nobutaka Hattori 3, Shigeki Aoki 1

1Department of Radiology, Juntendo University Graduate School of Medicine
2Department of Radiology, Juntendo University Graduate School of Medicine
3Department of Neurology, Juntendo University School of Medicine
4Department of Radiology, The University of Tokyo Graduate School of Medicine
5Department of Neurology, Juntendo University Nerima Hospital
6Department of Neurosurgery, Juntendo University School of Medicine

Abstract

Purpose

Micro fractional anisotropy (μFA) is more accurate than conventional fractional anisotropy (FA) for assessing microscopic tissue properties and can overcome limitations related to crossing white matter fibres. We compared μFA and FA for evaluating white matter changes in patients with Parkinson's disease (PD).

Methods

We compared FA and μFA measures between 25 patients with PD and 25 age- and gender-matched healthy controls using tract-based spatial statistics (TBSS) analysis. We also examined potential correlations between changes, revealed by conventional FA or μFA, and disease duration or unified Parkinson's disease rating scale (UPDRS)-III scores.

Results

Compared to healthy controls, patients with PD had significantly reduced μFA values, mainly in the anterior corona radiata (ACR). In the PD group, μFA values (primarily those from the ACR) were significantly negatively correlated with UPDRS-III motor scores. No significant changes or correlations with disease duration or UPDRS-III scores with tissue properties were detected using conventional FA.

Conclusions

μFA can evaluate microstructural changes that occur during white matter degeneration in patients with PD and may overcome a key limitation of FA.

Keywords • Parkinson's disease • Diffusion Tensor Imaging • Microscopic Fractional Anisotropy • Anterior Corona Radiata

Introduction

Parkinson's disease（PD）is a chronic and progressive neurodegenerative disorder characterised by motor symptoms (akinesia, resting tremor and rigidity) and a wide range of non-motor symptoms (such as olfactory dysfunction, cognitive impairment and depression) [1,2]. The diversity of motor and non-motor symptoms in patients with PD reflects the widespread progression of the underlying pathology, including the aggregation of α-synuclein immunoreactive inclusions in the form of Lewy pathologies within neuronal cytoplasm (Lewy bodies) and processes (Lewy neurites), loss of dopaminergic projections from the substantia nigra to the striatum and progressive loss of other neurotransmitter pathways, including cholinergic, noradrenergic and serotonergic [1-3].

The accumulation of Lewy pathology is likely associated with white matter degeneration in patients with PD [4,5]. Previous studies have used diffusion tensor imaging (DTI) for assessing white matter degeneration, as evidenced by decreased fractional anisotropy (FA) [6-9]. Despite its sensitivity, FA is not tissue-specific [10]. For example, decreased FA might result from changes in axon diameter, axon density or myelination. FA is also limited in areas with crossing fibres due to the influence of nerve fibre orientation within voxels. Specifically, this technique cannot represent multiple intra-voxel orientations [11].

Recently, a per-axon diffusion coefficient was proposed for analysing diffusion anisotropy in each nerve fibre. The micro FA (μFA) metric can evaluate neurodegeneration without influence from variations in nerve fibre orientations within the voxels [12]. Thus, μFA can overcome the problem of crossed fibres that limits FA derived from conventional DTI, and may emerge as a valuable biomarker for evaluating white matter *in vivo*.

We used μFA to assess microstructural white matter changes in patients with PD. We hypothesised that μFA would be a better measure than conventional FA for the detection of

microstructural white matter changes in patients with PD. To test our hypothesis, we compared measures obtained with conventional FA and μFA between healthy controls and patients with PD using tract-based spatial statistics (TBSS) analysis.

Materials and Methods

Subjects

Twenty-five patients with PD (mean age, 68.7 ± 8.72 years; 13 males) were included in this study. All patients with PD were diagnosed by movement disorders specialists based on the Movement Disorder Society's (MDS) clinical diagnostic criteria for PD [13] and were staged as I, II or III PD according to the Hoehn and Yahr scale. All patients with PD were taking levodopa in combination with a dopamine decarboxylase inhibitor (benserazide or carbidopa) at the time of MR imaging and clinical examination. Eighteen months or more after scanning, all patients with PD remained free of atypical parkinsonism and exhibited good responses to their respective anti-parkinsonian therapies. We also included 25 age- and gender-matched healthy controls (mean age, 68.0 ± 11.41 years; 13 males) with no history of neurologic or psychiatric disorders. The ethical committee of Juntendo University Hospital approved this study and written informed consent was obtained from all participants before evaluation. The demographic characteristics of the participants are shown in Table 1.

MR imaging

All MR images were obtained using a 3-T system (Achieva; Philips Healthcare, Best, the Netherlands) equipped with an eight-channel head coil for sensitivity-encoding parallel imaging. A spin-echo echo-planar imaging diffusion-weighted scheme was obtained and consisted of two b-values (1,000 and 2,000 s/mm^2) acquired along 32 uniformly distributed directions in an anterior-posterior phase encoding

direction. Each DWI acquisition was completed with a b = 0 image with no diffusion gradients. Standard and reverse phase encoded blipped images with no diffusion weighting (Blip Up and Blip Down) were also acquired to correct for magnetic susceptibility-induced distortions related to the EPI acquisitions [14]. The sequence parameters were as follows: image orientation, axial; repetition time (TR), 9810 ms, echo time (TE), 100 ms; diffusion gradient pulse duration (δ), 39.6 ms; diffusion gradient separation (Δ), 39.6 ms; field of view (FOV), 256 mm × 256 mm; matrix, 128 × 128; thickness, 2 mm and acquisition time, 5.14 min.

Diffusion MRI pre-processing

The diffusion-weighted data were corrected for susceptibility-induced geometric distortions, eddy current distortions and inter-volume subject motion using the EDDY and TOPUP toolboxes [14]. All DWI datasets were checked from 32 different axial, sagittal and coronal directions. All datasets were free from severe artefacts, such as gross geometric distortions, signal dropouts or bulk motion. μFA maps were obtained by fitting the model using the implementation from Kaden et al. [12], which is available at https://ekaden.github.io. The conventional diffusion tensor was estimated using the diffusion-weighted images with b = 0 and 1000 s/mm^2. We calculated FA for all subjects using the DTIFIT tool within the FMRIB Software Library 5.0.9 (FSL, Oxford Centre for Functional MRI of the Brain, UK; www.fmrib.ox.ac.uk/fsl) [15].

Tract-based spatial statistics (TBSS)

A voxel-wise statistical analysis was performed using TBSS implemented in FSL to regionally map significant between-group differences for FA and μFA. We also evaluated the relationship between each index and disease duration or UPDRS-III score. First, FA maps of all subjects were aligned to a standard

Montreal Neurological Institute (MNI152) space using the nonlinear registration tool FNIRT [16]. Second, the mean FA image was generated and thinned to create the mean FA skeleton (thresholded to FA > 0.20) that included the major white matter pathways, but excluded peripheral tracts and grey matter. Finally, the aligned FA map of each participant was projected onto this skeleton and assigning the maximum FA in a plane perpendicular to the local skeleton structure to each point on the skeleton. The same process was then applied to the μFA maps such that, without the initial registration, these maps were projected onto the mean FA.

Statistical analysis

All statistical analyses were performed using the Statistical Package for the Social Sciences for Windows, release 22.0 (SPSS, Chicago, IL), except for the general linear model (GLM) analysis where FSL was used. The Shapiro–Wilk test was used to assess data normality, whereas demographic data were analysed using the unpaired *t*-test and χ^2 test for continuous and categorical variables, respectively. Statistical significance for all two-tailed *P* values was set at 0.05.

For TBSS, the Randomise tool (FSL) was used to ascribe a family-wise error (FWE)–corrected *P* value (pFWE) to each cluster of voxels comprising the WM skeleton. The threshold-free cluster enhancement option was used in Randomise to avoid the selection of an arbitrary cluster-forming threshold, and 5,000 permutations were generated to provide an empirical null distribution of maximal cluster size. The voxel-wise statistics of the diffusion metrics for between-group differences (PD vs. healthy controls) were tested in the general linear model (GLM) framework using the unpaired t-test and the Randomise tool with nonparametric permutation testing. A pFWE of < 0.05 was considered significant for TBSS. The Randomise tool was also used to examine the relationship between diffusion metrics and disease duration, and the motor score of the unified PD rating scale (UPDRS)-III using

multiple linear regression analysis (pFWE < 0.05, corrected for gender and age).

Results

There were no significant differences in age ($P = 0.83$), or sex ($P = 1.00$) between patients with PD and healthy controls (Table 1).

TBSS analysis

μFA values were significantly reduced, mainly in the ACR and anterior thalamic radiation (ATR), in patients with PD compared to healthy controls (Fig. 1A, Table 2). In the PD group, μFA values (mainly from the ACR) showed a significant, negative correlation with UPDRS-III motor scores (Fig. 1B, Table 3). There were no significant between-group changes in FA and there was no significant correlation between FA and UPDRS-III score or between FA or μFA and disease duration.

Discussion

We compared μFA and conventional FA in patients with PD and healthy controls to examine the utility of μFA for evaluating the white matter microstructural changes that accompany PD. Compared with healthy controls, reduced μFA (predominantly in the ACR) was detected in patients with PD, whereas no significant changes were detected in conventional FA; thus, μFA seems to provide better sensitivity than conventional FA for detecting microstructural white matter changes in PD, especially in areas with crossing fibres. Our results are also supported by the fact that μFA was negatively correlated with UPDRS-III scores.

Our study demonstrates that compared with healthy controls, reduced μFA is predominantly

seen in the ACR of patients with PD. The ACR contains fibres that project from the brain stem to the prefrontal cortex via the internal capsule [17]. The prefrontal cortex is an area where Lewy-related pathologies, pathological hallmarks of PD, occur at a relatively early stage of the disease [18]. Lewy-related pathology is also evident within cerebral white matter, in parallel with cortical changes, and is associated with impaired axonal transport and subsequent microstructural changes in the axon [19]. Decreased μFA in the ACR likely reflects axonal pathology in the white matter of patients with PD. The finding is strengthened by a previous study that demonstrated a strong anticorrelation between μFA and axon diameter in fixed rat spinal cord, whereas only a moderate correlation between μFA and myelin water fraction [20]. However, a histological study is needed to confirm the relationship between μFA and axonal pathology in patients with PD. Furthermore, decreased μFA was observed in anterior thalamic radiation (ATR) and corona radiata areas and was significantly correlated with motor symptom scores. ATR and corona radiata areas contain fibre bundles connecting thalamocortical [21]. The disruption of thalamocortical networks has been shown to be closely related to the pathophysiology of PD and associated with motor symptoms, such as dyskinesia, in patients with PD [22-25]. Thus, decreased μFA in ATR and corona radiata in patients with PD in this study may also reflect the dysconnectivity of thalamocortical networks. Recently, the degeneration of thalamocortical network has also been characterized by the trigger psychiatric symptoms, such as hallucinations, delusions and cognitive impairments in patients with PD and dementia Lewy bodies (DLB) [26,27]. Higher MD in the sub-regions projecting from thalamus to prefrontal and parieto-occipital cortices was found in patients with DLB than the controls [28,29]. In addition, MD in the right thalamic sub-regions projecting to parietal and occipital cortices was significantly correlated with the severity scores of hallucinations [29]. Further, WM microstructural changes indicated by lower FA has been demonstrated in the ATR of patients with DLB [30]. Altogether, further studies using μFA may be required to clarify whether the pathology of PD is related to non-motor symptoms.

In this study, no significant difference was observed in FA in the ACR between patients with PD and healthy controls. In line with our results, Worker et al. [31] also reported no significant FA in the white matter of patients with PD. However, Kamagata et al. [23] and Taylor et al. [32] reported decreased FA in the corona radiata of patients with PD, compared with that of healthy controls. These conflicting results might be due to differences in sample size or disease stage. The discrepancy might also be due to the differences in disease duration. Of note, Kamagata et al. [23] and Taylor et al. [32] included patients with PD with a longer disease duration than that of our cohort or of the cohorts studied by Worker et al. [31] (mean disease duration, 7.1, 7.8, 7.0 and 6.6 years, respectively). Further, the ACR includes various fibre tracts that run in multiple directions, including the uncinate fasciculus, corpus callosum, inferior fronto-occipital fasciculus and anterior thalamic radiation, all of which contain many crossing fibres [33]. As mentioned above, FA is not appropriate to be used in the evaluation of white matter with crossing fibres because FA is dependent on both the microscopic anisotropy and orientation dispersion [34]. The presence of crossing fibres will consequently reduce FA by inducing a higher degree of orientation dispersion [35,36], or selective damage to one of the fibre populations in the region will result in reduced orientation dispersion and elevated FA [37]. Thus, the utility of FA as a measure of white matter integrity in neurodegenerative diseases such as PD may be less reliable. Conversely, the effect of orientation dispersion has been removed from the quantification of microscopic anisotropy in the calculation of μFA, making it a more direct measure of white matter tissue structure on the microscopic scale [37,38]. Previous studies have demonstrated that μFA has higher sensitivity than FA for the detection of microstructural changes [38,39]. Additionally, FA has been shown to be insensitive to the condition in which tissue damage occurs in randomly oriented components, whereas μFA reflects the amount of microscopic anisotropy that is lost [37]. Overall, our study supports the notion that μFA is superior to FA in the evaluation of white matter microstructural changes in patients with PD. A further study with an earlier-stage PD cohort is needed to confirm the sensitivity of μFA in PD pathology.

Limitations

First, we examined a relatively small cohort of patients with PD. Multi-centre and larger sample size studies are needed to establish μFA as a biomarker for white matter microstructural changes in patients with PD. Second, the diagnosis of PD lacked histopathological verification. However, the diagnosis was strengthened by the fact that all patients with PD consistently exhibited a good response to antiparkinsonian therapy and remained free of atypical parkinsonism after being followed for 18 months or more. Third, this study did not evaluate non-motor symptoms of patients with PD. PD is a complex neurodegenerative disease with broad-spectrum motor and non-motor symptoms and is often associated with non-motor symptoms, such as cognitive deficits [40]. Therefore, future MRI studies should evaluate the relationships between μFA changes and clinical non-motor symptoms of patients with PD. Fourth, control subjects did not undergo detailed cognitive evaluation, such as MMSE. However, all control subjects underwent neurological examination by neurology specialists, and cognitive decline cases were excluded. Fifth, besides μFA, other advanced diffusion MRI techniques, such as diffusional kurtosis imaging (DKI) [41], neurite orientation density and dispersion imaging (NODDI) [42], have also been proposed as means of evaluating neurodegeneration in regions that contain many crossing fibres. Further studies that compare these methods will be of great interest. Lastly, we used commonly available single diffusion encoding (SDE) [43] methodology and the spherical mean technique (SMT) [12,44], consisting of powder‐averaged SDE signals and imposition of constraints in this study. The constraints of SMT [12,44], such as fixed diffusivity, can lead to biased quantification. Recently, double diffusion encoding (DDE) using two independently pulsed gradient vectors that probe correlations in water diffusion in different directions has been introduced for more accurate quantification of μA and to overcome various limitations of the other method. To this end, DDE has showed promising results [45,46]. Further studies that use DDE instead of SDE may allow for more accurate estimation of white matter *in vivo*.

Conclusion

μFA can be used to evaluate microstructural white matter degeneration-related changes in patients with PD and may overcome the limitation of FA with regard to crossing fibres. μFA might also be useful for evaluating disease progression in patients with PD.

References

1. Fearnley JM, Lees AJ (1991) Ageing and Parkinson's disease: substantia nigra regional selectivity. Brain 114 (Pt 5):2283-2301

2. Schapira AHV, Chaudhuri KR, Jenner P (2017) Non-motor features of Parkinson disease. Nat Rev Neurosci 18 (7):435-450. doi:10.1038/nrn.2017.62

3. Braak H, Del Tredici K, Rub U, de Vos RA, Jansen Steur EN, Braak E (2003) Staging of brain pathology related to sporadic Parkinson's disease. Neurobiol Aging 24 (2):197-211

4. Braak H, Bohl JR, Muller CM, Rub U, de Vos RA, Del Tredici K (2006) Stanley Fahn Lecture 2005: The staging procedure for the inclusion body pathology associated with sporadic Parkinson's disease reconsidered. Mov Disord 21 (12):2042-2051. doi:10.1002/mds.21065

5. Kanazawa T, Adachi E, Orimo S, Nakamura A, Mizusawa H, Uchihara T (2012) Pale neurites, premature alpha-synuclein aggregates with centripetal extension from axon collaterals. Brain Pathol 22 (1):67-78. doi:10.1111/j.1750-3639.2011.00509.x

6. Hattori T, Orimo S, Aoki S, Ito K, Abe O, Amano A, Sato R, Sakai K, Mizusawa H (2012) Cognitive status correlates with white matter alteration in Parkinson's disease. Hum Brain Mapp 33 (3):727-739. doi:10.1002/hbm.21245

7. Kamagata K, Motoi Y, Abe O, Shimoji K, Hori M, Nakanishi A, Sano T, Kuwatsuru R, Aoki S, Hattori N (2012) White matter alteration of the cingulum in Parkinson disease with and without dementia: evaluation by diffusion tensor tract-specific analysis. AJNR Am J Neuroradiol 33 (5):890-895. doi:10.3174/ajnr.A2860

8. Kamagata K, Motoi Y, Tomiyama H, Abe O, Ito K, Shimoji K, Suzuki M, Hori M, Nakanishi A, Sano T, Kuwatsuru R, Sasai K, Aoki S, Hattori N (2013) Relationship between cognitive impairment and white-matter alteration in Parkinson's disease with dementia: tract-based spatial statistics and tract-specific analysis. Eur Radiol 23 (7):1946-1955. doi:10.1007/s00330-013-2775-4

9. Karagulle Kendi AT, Lehericy S, Luciana M, Ugurbil K, Tuite P (2008) Altered diffusion in the frontal lobe in Parkinson disease. AJNR Am J Neuroradiol 29 (3):501-505. doi:10.3174/ajnr.A0850

10. Assaf Y, Pasternak O (2008) Diffusion tensor imaging (DTI)-based white matter mapping in brain research: a review. J Mol Neurosci 34 (1):51-61. doi:10.1007/s12031-007-0029-0

11. Alexander AL, Lee JE, Lazar M, Field AS (2007) Diffusion tensor imaging of the brain. Neurotherapeutics 4 (3):316-329. doi:10.1016/j.nurt.2007.05.011

12. Kaden E, Kruggel F, Alexander DC (2016) Quantitative mapping of the per-axon diffusion coefficients in brain white matter. Magnetic resonance in medicine 75 (4):1752-1763. doi:10.1002/mrm.25734

13. Postuma RB, Berg D, Stern M, Poewe W, Olanow CW, Oertel W, Obeso J, Marek K, Litvan I, Lang AE, Halliday G, Goetz CG, Gasser T, Dubois B, Chan P, Bloem BR, Adler CH, Deuschl G (2015) MDS clinical diagnostic criteria for Parkinson's disease. Mov Disord 30 (12):1591-1601. doi:10.1002/mds.26424

14. Andersson JL, Sotiropoulos SN (2016) An integrated approach to correction for off-resonance effects and subject movement in diffusion MR imaging. Neuroimage 125:1063-1078. doi:10.1016/j.neuroimage.2015.10.019

15. Basser PJ, Mattiello J, LeBihan D (1994) Estimation of the effective self-diffusion tensor from the NMR spin echo. J Magn Reson B 103 (3):247-254

16. Jenkinson M, Beckmann CF, Behrens TE, Woolrich MW, Smith SM (2012) Fsl. Neuroimage 62 (2):782-790. doi:10.1016/j.neuroimage.2011.09.015

17. Mancall EL, Brock DG, Gray H (2011) Gray's clinical neuroanatomy: the anatomic basis for clinical neuroscience. Elsevier/Saunders.

18. Braak H, Del Tredici K (2008) Invited Article: Nervous system pathology in sporadic Parkinson disease. Neurology 70 (20):1916-1925. doi:10.1212/01.wnl.0000312279.49272.9f

19. Duncan GW, Firbank MJ, Yarnall AJ, Khoo TK, Brooks DJ, Barker RA, Burn DJ, O'Brien JT (2016) Gray and white matter imaging: A biomarker for cognitive impairment in early Parkinson's disease? Mov

Disord 31 (1):103-110. doi:10.1002/mds.26312

20. Shemesh N (2018) Axon and myelin content modulate microscopic fractional anisotropy at short diffusion times in fixed rat spinal cord. Front Phys 6 (49). doi:10.3389/fphy.2018.00049

21. Nieuwenhuys R, Voogd J, van Huijzen C (2008) The human central nervous system: a synopsis and atlas. Spr Sci Business Media doi:10.1007/978-3-540-34686-9

22. Ji GJ, Hu P, Liu TT, Li Y, Chen X, Zhu C, Tian Y, Chen X, Wang K (2018) Functional connectivity of the corticobasal ganglia-thalamocortical network in Parkinson disease: A systematic review and meta-analysis with cross-validation. Radiology 287 (3):973-982. doi:10.1148/radiol.2018172183

23. Kamagata K, Zalesky A, Hatano T, Di Biase MA, El Samad O, Saiki S, Shimoji K, Kumamaru KK, Kamiya K, Hori M, Hattori N, Aoki S, Pantelis C (2018) Connectome analysis with diffusion MRI in idiopathic Parkinson's disease: Evaluation using multi-shell, multi-tissue, constrained spherical deconvolution. Neuroimage Clin 17:518-529. doi:10.1016/j.nicl.2017.11.007

24. Long Z, Xu Q, Miao HH, Yu Y, Ding MP, Chen H, Liu ZR, Liao W (2017) Thalamocortical dysconnectivity in paroxysmal kinesigenic dyskinesia: Combining functional magnetic resonance imaging and diffusion tensor imaging. Mov Disord 32 (4):592-600. doi:10.1002/mds.26905

25. Rodriguez-Oroz MC, Jahanshahi M, Krack P, Litvan I, Macias R, Bezard E, Obeso JA (2009) Initial clinical manifestations of Parkinson's disease: features and pathophysiological mechanisms. Lancet Neurol 8 (12):1128-1139. doi:10.1016/S1474-4422(09)70293-5

26. Esmaeeli S, Murphy K, Swords GM, Ibrahim BA, Brown JW, Llano DA (2019) Visual hallucinations, thalamocortical physiology and Lewy body disease: A review. Neurosci Biobehav Rev 103:337-351. doi:10.1016/j.neubiorev.2019.06.006

27. Onofrj M, Espay AJ, Bonanni L, Delli Pizzi S, Sensi SL (2019) Hallucinations, somatic-functional disorders of PD-DLB as expressions of thalamic dysfunction. Mov Disord 34 (8):1100-1111. doi:10.1002/mds.27781

28. Delli Pizzi S, Franciotti R, Taylor JP, Thomas A, Tartaro A, Onofrj M, Bonanni L (2015) Thalamic involvement in fluctuating cognition in dementia with Lewy bodies: Mag Res Evidences. Cereb Cortex 25 (10):3682-3689. doi:10.1093/cercor/bhu220

29. Delli Pizzi S, Maruotti V, Taylor JP, Franciotti R, Caulo M, Tartaro A, Thomas A, Onofrj M, Bonanni L (2014) Relevance of subcortical visual pathways disruption to visual symptoms in dementia with Lewy bodies. Cortex 59:12-21. doi:10.1016/j.cortex.2014.07.003

30. Delli Pizzi S, Franciotti R, Taylor JP, Esposito R, Tartaro A, Thomas A, Onofrj M, Bonanni L (2015) Structural connectivity is differently altered in dementia with Lewy body and Alzheimer's disease. Front Aging Neurosci 7:208. doi:10.3389/fnagi.2015.00208

31. Worker A, Blain C, Jarosz J, Chaudhuri KR, Barker GJ, Williams SC, Brown RG, Leigh PN, Dell'Acqua F, Simmons A (2014) Diffusion tensor imaging of Parkinson's disease, multiple system atrophy and progressive supranuclear palsy: a tract-based spatial statistics study. PLoS One 9 (11):e112638. doi:10.1371/journal.pone.0112638

32. Taylor KI, Sambataro F, Boess F, Bertolino A, Dukart J (2018) Progressive decline in gray and white matter integrity in de novo Parkinson's disease: An analysis of longitudinal Parkinson progression markers initiative diffusion tensor imaging data. Front Aging Neurosci 10:318. doi:10.3389/fnagi.2018.00318

33. Mori S, Wakana S, Van Zijl PCM (2005) MRI atlas of human white matter. 1st edn. Elsevier, Amsterdam, The Netherlands; Boston

34. Nilsson M, Szczepankiewicz F, Topgaard D Quantification of microscopic anisotropy with diffusion MRI. Front Neurosci. doi:10.3389/conf.fnins.2015.88.00004

35. Alexander AL, Hasan KM, Lazar M, Tsuruda JS, Parker DL (2001) Analysis of partial volume effects in diffusion-tensor MRI. Magn Reson Med 45 (5):770-780

36. Nilsson M, Latt J, Stahlberg F, van Westen D, Hagslatt H (2012) The importance of axonal undulation in diffusion MR measurements: a Monte Carlo simulation study. NMR Biomed 25 (5):795-805.

doi:10.1002/nbm.1795

37. Szczepankiewicz F, Lasic S, van Westen D, Sundgren PC, Englund E, Westin CF, Stahlberg F, Latt J, Topgaard D, Nilsson M (2015) Quantification of microscopic diffusion anisotropy disentangles effects of orientation dispersion from microstructure: applications in healthy volunteers and in brain tumors. Neuroimage 104:241-252. doi:10.1016/j.neuroimage.2014.09.057

38. Lawrenz M, Brassen S, Finsterbusch J (2016) Microscopic diffusion anisotropy in the human brain: Age-related changes. Neuroimage 141:313-325. doi:10.1016/j.neuroimage.2016.07.031

39. Lawrenz M, Brassen S, Finsterbusch J (2015) Microscopic diffusion anisotropy in the human brain: reproducibility, normal values, and comparison with the fractional anisotropy. Neuroimage 109:283-297. doi:10.1016/j.neuroimage.2015.01.025

40. Muslimovic D, Post B, Speelman JD, Schmand B (2005) Cognitive profile of patients with newly diagnosed Parkinson disease. Neurology 65 (8):1239-1245. doi:10.1212/01.wnl.0000180516.69442.95

41. Jensen JH, Helpern JA, Ramani A, Lu H, Kaczynski K (2005) Diffusional kurtosis imaging: the quantification of non-gaussian water diffusion by means of magnetic resonance imaging. Mag Res Med 53 (6):1432-1440. doi:10.1002/mrm.20508

42. Zhang H, Schneider T, Wheeler-Kingshott CA, Alexander DC (2012) NODDI: practical in vivo neurite orientation dispersion and density imaging of the human brain. NeuroImage 61 (4):1000-1016. doi:10.1016/j.neuroimage.2012.03.072

43. Shemesh N, Jespersen SN, Alexander DC, Cohen Y, Drobnjak I, Dyrby TB, Finsterbusch J, Koch MA, Kuder T, Laun F, Lawrenz M, Lundell H, Mitra PP, Nilsson M, Ozarslan E, Topgaard D, Westin CF (2016) Conventions and nomenclature for double diffusion encoding NMR and MRI. Magn Reson Med 75 (1):82-87. doi:10.1002/mrm.25901

44. Kaden E, Kelm ND, Carson RP, Does MD, Alexander DC (2016) Multi-compartment microscopic diffusion imaging. Neuroimage 139:346-359. doi:10.1016/j.neuroimage.2016.06.002

45. Henriques RN, Jespersen SN, Shemesh N (2019) Microscopic anisotropy misestimation in spherical-mean single diffusion encoding MRI. Magn Reson Med 81 (5):3245-3261. doi:10.1002/mrm.27606

46. Ianus A, Jespersen SN, Serradas Duarte T, Alexander DC, Drobnjak I, Shemesh N (2018) Accurate estimation of microscopic diffusion anisotropy and its time dependence in the mouse brain. Neuroimage 183:934-949. doi:10.1016/j.neuroimage.2018.08.034

Figure legends

Fig. 1 Comparison of conventional FA and μFA indices between healthy controls and patients with PD

A. TBSS analyses showed that patients with PD had significantly lower μFA (blue/light-blue voxels) than healthy controls ($P < 0.05$, FWE-corrected). B. TBSS analysis also showed a significant correlation between μFA and UPDRS-III (cool voxels) ($P < 0.05$, FWE-corrected). The skeleton is presented in green. To aid visualisation, the results have been thickened using the fill script implemented in the FMRIB Software Library. FA, fractional anisotropy; μFA, micro FA; PD, Parkinson's disease; TBSS, tract-based spatial statistics; UPDRS-III, unified Parkinson's disease rating scale-III

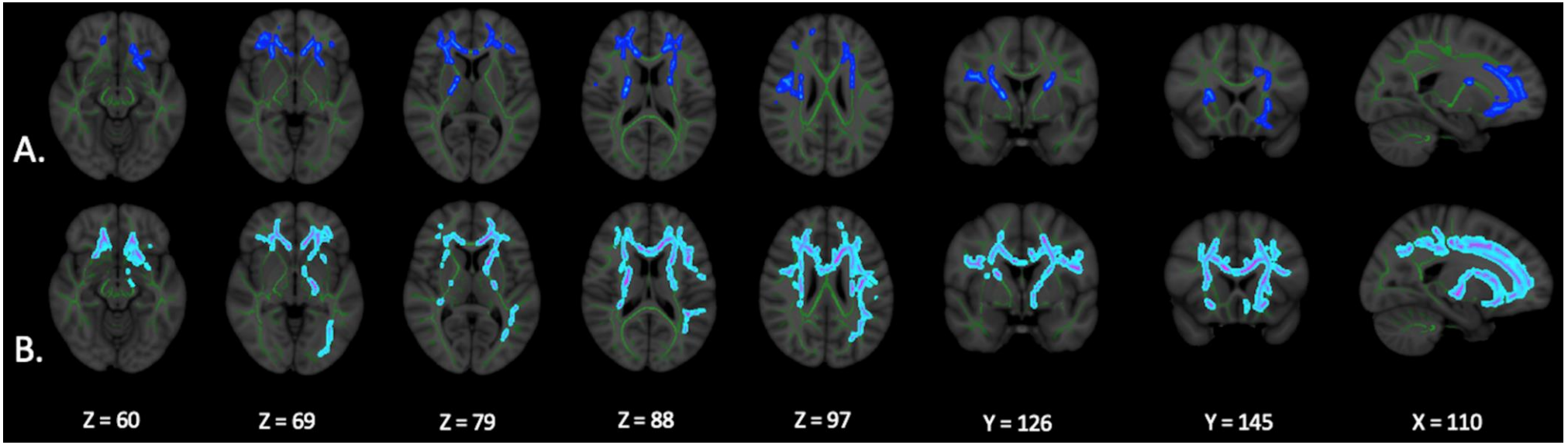

Figure 1

Table 1. Demographic characteristics of subjects

	Healthy controls	PD patients	*P*-value
Number	25	25	N/A
Sex (male:female)	13:12	13:12	1.00
Age in years, mean (SD)	68.0 (11.4)	68.7 (8.7)	0.83
Disease duration in years, mean (SD)	N/A	7.0 (4.4)	N/A
Hoehn–Yahr stage, mean (SD)	N/A	2.1 (0.7)	N/A
UPDRS-III motor score, mean (SD)	N/A	16.2 (8.6)	N/A
MMSE score, mean (SD)*	N/A	28.22 (2.29)	N/A
Duration of medication in months, mean (SD)	N/A	58.92 (45.62)	N/A

MMSE, mini-mental state exam; N/A, not applicable; PD, Parkinson's disease; SD, standard deviation; UPDRS-III, Unified Parkinson's Disease Rating Scale-III *Only available for 22 PD patients.

Table 2. Tract-based spatial statistics analysis of μFA in patients with Parkinson's disease and healthy controls.

Modality	**Contrast**	**Cluster size**	**Anatomical region**	**Peak *t*-value**	**Peak MNI coordinates (*X*, *Y*, *Z*)**
μFA	HCs > PDs	6002	Bilateral anterior thalamic radiation, inferior fronto–occipital fasciculus, anterior limb of internal capsule, anterior and superior corona radiata; Right corticospinal tract, superior longitudinal fasciculus, posterior limb of internal capsule; Left uncinate fasciculus; Forceps minor, genu and body of corpus callosum	4	70, 169, 78

μFA, micro fractional anisotropy; HCs, healthy controls; PDs, patients with Parkinson's disease

Table 3. Tract-based spatial statistics analysis of μFA and UPDRS-III in patients with Parkinson's disease.

Modality	**Contrast**	**Cluster size**	**Anatomical region**	**Peak *t*-value**	**Peak MNI coordinates (*X*, *Y*, *Z*)**
μFA	Negative correlation with UPDRS-III	17682	Bilateral anterior thalamic radiation, corticospinal tract, cingulum cingulate gyrus, inferior fronto-occipital fasciculus, superior longitudinal fasciculus, uncinate fasciculus, anterior and posterior limb and retrolenticular part of internal capsule, anterior, superior, and posterior corona radiata; Left inferior longitudinal fasciculus, superior longitudinal fasciculus temporal part, and cerebral peduncle; forceps minor, genu, body, and splenium of corpus callosum	5.17	111, 162, 67

μFA, micro fractional anisotropy; UPDRS-III, Unified Parkinson's Disease Rating Scale-III